Searching for Supersymmetry with the α_T variable in $p\bar{p}$ collisions with the CMS Detector at the Large Hadron Collider

Zoe Hatherell

A thesis submitted in fulfilment of the requirements
for the degree of Doctor of Philosophy
to Imperial College London
December 2011

Abstract

Declaration

Except where otherwise stated, the research undertaken in this thesis was the unaided work of the author. Where the work was done in collaboration with others, a significant contribution was made by the author.

Z. Hatherell
December 2011

Acknowledgements

I would like to record my thanks to all those who have helped me in the course of this work. In particular, the following:

Contents

List of Figures

List of Tables

Chapter 1

Introduction

Describe storyline of Thesis.

Chapter 2

Theoretical Overview

2.1 The Standard Model

2.2 Motivation for New Physics

2.3 Supersymmetry

Chapter 3

The Compact Muon Solenoid Experiment at the LHC

3.1 The Large Hadron Collider

The Large Hadron Collider (LHC) is a circular synchrotron of circumference 27km designed to collide proton beams with a centre of mass energy $\sqrt{s} = 14\,\text{TeV}$ at a final design luminosity of $10^{34}\text{cm}^{-2}\text{s}^{-1}$, with the aim of discovering new physics at the TeV scale.

3.2 The Compact Muon Solenoid

The Compact Muon Solenoid (CMS) is one of the two multi-purpose detectors at the LHC, designed to capitalise on the full range of physics opportunities available at the LHC. These goals are pursued through the design and construction of the detector and development of software for the reconstruction of physics objects. The detector is constructed of several detector sub-systems contained inside and wrapped in layers around a central 13m long 4T super conducting solenoid as shown in Figure 3.1.

The high magnetic field was chosen in order to achieve the bending power necessary for good charged particle momentum resolution. The inner bore of the solenoid is large enough that the inner tracker and the calorimeters are located inside, which minimises the material the partials pass through before entering the calorimeters. This allows a good energy measurement. Four muon "stations"

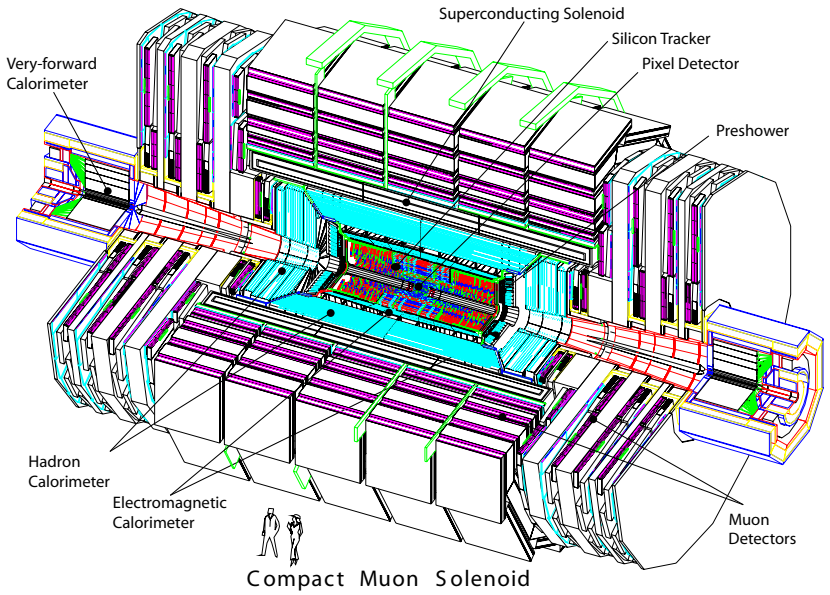

Figure 3.1: A cutaway diagram of the CMS detector structure identifying the main individual sub-systems.

of aluminium drift tubes are integrates within the iron magnetic field return yoke. The full design description can be found in the CMS Technical Design Proposal [1]. As different particles pass through the detector they interact in the sub-systems depending on their type. A transverse slice through the detector illustrating the path through the machine of each type of particle is shown in Figure 3.2

3.2.1 Coordinate System

The coordinate system chosen by CMS uses the nominal interaction point within the detector as the origin. The x-axis points radially inwards to the centre of the beam pipe, and the y-axis points vertically upward. The z-axis then points in the direction of the beam. The azimuthal angle ϕ is defined as the angle from the x-axis in the x-y plane, and the polar angle θ from the z-axis. However, it is common convention to express θ in terms of the Lorentz Invariant quantity, pseudorapidity $\eta = -\ln\tan(\theta/2)$, as particle production is approximately uniform in η. The transverse components of the energy and momentum, denoted E_T and p_T are then calculated form the x and y components.

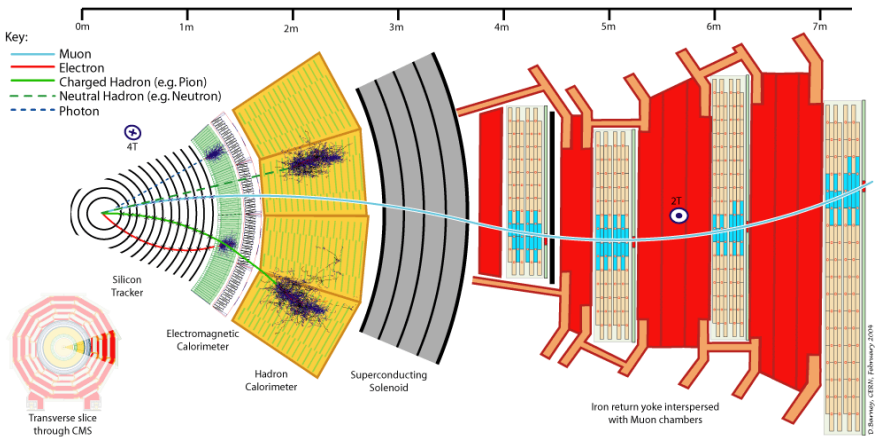

Figure 3.2: Transverse slice through the CMS Detector showing each type of particle and how it interacts with the sub-detectors.

3.2.2 Tracker

3.2.3 ECAL

Immediately outside of the tracker, and still within the magnet core, sits the Electromagnetic Calorimeter (ECAL), used to measure the energy of electrons, photons and pions via the energy they lose through radiation. Electrons lose their energy in the material through bremsstrahlung, and photons by decaying to an electron-positron pair. Using a hermetic homogenous calorimeter of scintillating crystals, this energy can be converted to scintillation light which is picked up by a light sensitive detector.

The use of high density crystals allows a fast calorimeter which has fine granularity and is radiation resistant, requirements which are essential in the LHC environment. After rigorous research and development, lead tungstate ($PbWO_4$) crystals were chosen as the optimal solution to the requirements of LHC operation, due to a number of desirable characteristics. The extremely short radiation length $X_0 = 0.89$cm allows the construction of a compact ECAL which therefore can reside within the solenoid, hence reducing the layers of material the particles have already passed through. In addition, the material has a low Moliere radius (2.2cm) meaning the transverse size of the electromagnetic shower is small, leading to good shower position resolution and separation. It is also essential that a fast scintillator is used, in order to distinguish between bunch crossings. In crystals of $PbWO_4$ 80% of the scintillation light is emitted within

25ns, the bunch spacing of the LHC. Finally the crystals are hard to radiation, as their method of scintillation is resistant to radiation damage.

The ECAL is structurally divided into three distinct regions, the Endcaps (EE), the Barrel (EB) and the Preshower (PS), which together cover a pseudo-rapidity range $|\eta| \leq 3$. The ECAL Barrel is a cylindrical arrangement of 61200 $PbWO_4$ crystals covering the pseudo rapidity range $|\eta| \leq 1.479$ with a granularity of $\Delta\eta \times \Delta\phi = 0.0174 \times 0.0174$. The radius to the front-face of the crystals is 1.29 m.

The ECAL is closed by two identical endcap regions, which cover the range $1.479 \leq |\eta| \leq 3$ at the margins of the barrel, and consist of 7324 crystals each. Both are divided into two halved, or *Dees* Precision energy measurements are possible up to $|\eta| = 2.6$, but crystals are include up to $|\eta| = 3$ to assist the forward-direction energy-flow measurement. The end cap crystals are also wedge shaped with a square front face $28.62 \times 28.62 mm^2$ and a square back face $30 \times 30 mm^2$. The crystals point slightly away from the interaction point in order to make the end-caps hermetic, and are grouped mechanically into 5×5 super-crystals (SC).

The size of the crystals is chosen to reflect the properties and requirements, such that the front face surface area is 22mm x 22mm (the size of the Moliere radius) and the longitudinal depth of the crystals is 230mm, which is 25.8 X_0 in the barrel, hence allowing a fine granularity and a compact ECAL. In the end-caps the presence of the PS allows for shorter crystals, of 220m, corresponding to 24.7 X_0.

A additional component, the Pre-Shower is present in front of the end-caps covering a range of $1.653 \leq |\eta| \leq 2.6$ and consists of two layers of absorbing lead converters and silicon detectors. The primary function of the PS is to identify neutral pions that decay into two photons in the end-caps, which can fake a high-energy photon. It also possesses a high granularity, and therefore is used to improve position determination of particles, and helps the identification of electrons against minimum ionising particles. The two layers of the PS have their strips orthogonal to one another such that the first layer has vertical strips to measure the critical position, and the second horizontal strips for the horizontal position.

The scintillators are read out using photodetectors, which convert the scintillating light of the crystals into an electric signal. The crystals were chosen

by a rigorous optimisation of the properties required, which results in a high-performance ECAL, however this material has a relatively low light yield. In order to overcome this, photodetectors designed for use in a magnetic field with intrinsic gain are used. Vacuum Phototriodes (VPTs) are used in the end-caps. These are unsuitable in the central region due to high magnetic, but due to lower radiation levels Avalanche Photodiodes (APDs) are used. Both the crystals and the photodetectors are sensitive to temperature changes, so a stable temperature must be maintained. Radiation damage to the crystals decreases with temperature, but so do the thermal effects which result in recovery. The operational temperature, 18C is chosen as it is the point of equilibrium between damage and recovery.

The resolution of an ECAL can be described as a function of the energy E in GeV, shown in Equation: 3.1, for energies below about 500 GeV. Above this shower leakage from the back of the crystals become non-negligible.

$$\left(\frac{\sigma}{E}\right)^2 = \left(\frac{S}{\sqrt{E}}\right)^2 + \left(\frac{N}{E}\right)^2 + C^2 \tag{3.1}$$

The stochastic term S represents fluctuations related to statistics, including photoelectron statistics and intrinsic shower variations. The noise term N takes into account electronic noise summed over readout channels, and the constant term C accounts for the uncertainty in calibration and the detector non-uniformity. Measurements from test beam reconstructed energy distributions show values for the terms to be $S = 2.8 \pm 0.1\,\%$, N=0.12 GeV and $C = 0.30 \pm 0.01\,\%$.

3.2.4 HCAL

3.2.5 Magnet

3.2.6 Muons

3.2.7 Trigger

Reconstruction

Chapter 4

SUSY Search Topology and the α_T variable

4.1 SUSY Search Toplogies

4.2 α_T in a di-jet system

4.3 α_T in a n-jet system

4.4 α_T search strategy

Chapter 5

The all-hadronic search with inclusive jets + missing energy

5.1 Event Selection

5.2 Analysis and Results

5.3 Data-Driven Background Estimation

5.3.1 Total background prediction

5.3.2 Estimating EWK background using high p_T using W+Jets events

5.3.3 Estimation Z $\nu\bar{\nu}$ + jets background using photon + jets events

5.4 Systematic Uncertainties

5.5 Limits

5.6 Conclusion

Chapter 6

Using the α_T method in single lepton search

6.1 Extending the α_T approach in events with one lepton, jets and missing energy

6.2 Event Selection

6.3 Analysis and Results

6.4 Data-Driven Background Estimation

6.4.1 Total background prediction in HT bins

6.5 Systematic Uncertainties

6.6 Limits

6.7 Conclusion

Chapter 7

Conclusions

Bibliography

[1] The CMS Collaboration. The Compact Muon Solenoid Technical Proposal. *CERN/LHCC*, 94-38, 1994.